Mechanical Faraday effect for orbital angular momentum-carrying beams

Emma Wisniewski-Barker,[1*] **Graham M. Gibson,**[1]
Sonja Franke-Arnold,[1] **Robert W. Boyd,**[1,2,3] **and Miles J. Padgett**[1]

[1]*University of Glasgow, Department of Physics and Astronomy, SUPA, Glasgow, UK*
[2]*University of Rochester, The Institute of Optics and Department of Physics and Astronomy, Rochester, New York 14627, USA*
[3]*University of Ottawa, Department of Physics, Ottawa, Ontario, Canada*
**e.wisniewski-barker.1@research.gla.ac.uk*

Abstract: When linearly polarised light is transmitted through a spinning window, the plane of polarisation is rotated. This rotation arises through a phase change that is applied to the circularly polarised states corresponding to the spin angular momentum (SAM). Here we show an analogous effect for the orbital angular momentum (OAM), where a differential phase between the positive and negative modes ($\pm\ell$) is observed as a rotation of the transmitted image. For normal materials, this rotation is on the order of a micro radian, but by using a slow-light medium, we show a rotation of a few degrees. We also note that, within the bounds of our experimental parameters, this rotation angle does not exceed the scale of the spatial features in the beam profile.

OCIS codes: (190.4400) Nonlinear optics, materials; (350.5500) Propagation.

References and links

1. M. Faraday, "Experimental researches in electricity - nineteenth series," Philos. T. R. Soc. Lond. **136**, 1–20 (1846).
2. J. G. Dawber, "The Faraday effect, magnetic rotatory dispersion and magnetic circular dichroism," Analyst **89**, 755–762 (1964).
3. G. Nienhuis, J. P. Woerdman, and I. Kuscer, "Magnetic and mechanical Faraday effects," Phys. Rev. A **46**, 7079–7092 (1992).
4. M. J. Padgett, G. Whyte, J. Girkin, A. Wright, L. Allen, P. Öhberg, and S. M. Barnett, "Polarization and image rotation induced by a rotating dielectric rod: an optical angular momentum interpretation," Opt. Lett. **31**, 2205–2207 (2006).
5. L. Allen and M. J. Padgett, "Equivalent geometric transformations for spin and orbital angular momentum of light," J. Mod. Opt. **54**, 487–491 (2007).
6. J. B. Götte, S. M. Barnett, and M. J. Padgett, "On the dragging of light by a rotating medium," Proc. Roy. Soc. Lond. A **463**, 2185–2194 (2007).
7. R. V. Jones, "Rotary 'aether drag'," Proc. Roy. Soc. Lond. A **349**, 423–439 (1976).
8. L. Allen, M. Beijersbergen, R. Spreeuw, and J. Woerdman, "Orbital angular momentum of light and the transformation of Laguerre-Gaussian laser modes," Phys. Rev. A **45**, 8185–8189 (1992).
9. A. M. Yao and M. J. Padgett, "Orbital angular momentum: origins, behavior and applications," Adv. Opt. Photon. **3**, 161–204 (2011).
10. M. J. Padgett and J. Courtial, "Poincare-sphere equivalent for light beams containing orbital angular momentum," Opt. Lett. **24**, 430–432 (1999).
11. R. Jones, "'Fresnel aether drag' in a transversely moving medium," Proc. Roy. Soc. Lond. A **328**, 337–352 (1972).
12. M. A. Player, "On the dragging of the plane of polarization of light propagating in a rotating medium," Proc. Roy. Soc. Lond. A **349**, 441–445 (1976).

#206677 - $15.00 USD Received 18 Feb 2014; revised 30 Mar 2014; accepted 23 Apr 2014; published 7 May 2014

13. J. Leach, A. Wright, J. Götte, J. Girkin, L. Allen, S. Franke-Arnold, S. M. Barnett, and M. J. Padgett, "'Aether drag' and moving images," Phys. Rev. Lett. **100**, 153902 1–4 (2008).
14. M. S. Bigelow, N. N. Lepeshkin, and R. W. Boyd, "Observation of ultraslow light propagation in a ruby crystal at room temperature," Phys. Rev. Lett. **90**, 113903 1–4 (2003).
15. M. S. Bigelow, N. N. Lepeshkin, and R. W. Boyd, "Superluminal and slow light propagation in a room temperature solid," Science **301**, 200–202 (2003).
16. S. Franke-Arnold, G. Gibson, R. W. Boyd, and M. J. Padgett, "Rotary photon drag enhanced by a slow-light medium," Science **333**, 65–67 (2011).
17. R. W. Boyd, "Slow and fast light: fundamentals and applications," J. Mod. Opt. **56**, 1908–1915 (2009).
18. J. Courtial, K. Dholakia, D. A. Robertson, L. Allen, and M. J. Padgett, "Measurement of the rotational frequency shift imparted to a rotating light beam possessing orbital angular momentum," Phys. Rev. Lett. **80**, 3217–3219 (1998).
19. S. Franke-Arnold, J. Leach, M. J. Padgett, V. E. Lembessis, D. Ellinas, A. J. Wright, J. M. Girkin, P. Ohberg, and A. S. Arnold, "Optical ferris wheel for ultracold atoms," Opt. Express **15**, 8619–8625 (2007).
20. E. Wisniewski-Barker, G. Gibson, S. Franke-Arnold, Z. Shi, R. W. Boyd, and M. J. Padgett, "Evidence of slow-light effects from rotary drag of structured beams," New J. Phys. **15**, 083020 (2013).
21. G. G. Kozlov, S. V. Poltavtsev, I. I. Ryzhov, and V. S. Zapasskii, "Comment on 'Evidence of slow-light effects from rotary drag of structured beams'," New J. Phys. **16**, 038001 (2014).
22. E. Wisniewski-Barker, G. Gibson, S. Franke-Arnold, Z. Shi, R. W. Boyd, and M. J. Padgett, "Reply to comment on 'Evidence of slow-light effects from rotary drag of structured beams'," New J. Phys. **16**, 038002 (2014).
23. E. B. Aleksandrov, V. S. Zapasskii, "A saturable absorber, coherent population oscillations, and slow light," Phys. Usp. **49**, 1067–1075 (2006).

The magnetic Faraday effect is a well-known phenomenon that occurs when a light beam passes through a medium subject to a magnetic field, and it has been studied for over a century [1–3]. The component of the magnetic field in the direction of the light propagation causes a rotation of the polarisation state of the light. This magneto-optical effect has a mechanical analogy, known as the mechanical Faraday effect, where the rotation of a medium causes a rotation of the polarisation state of the light passing through it [4–6]. Polarisation rotation through the mechanical Faraday effect was first observed by Jones in 1976 [7]. In the mechanical Faraday effect, the rotation of linear polarisation arises from a phase shift between the right- and left-circularly polarised light that is superimposed to create linearly polarised light. Polarisation can be represented visually on a Poincaré sphere, as seen in Fig. 1(a) and is associated with a spin angular momentum (SAM) of $\pm\hbar$ per photon.

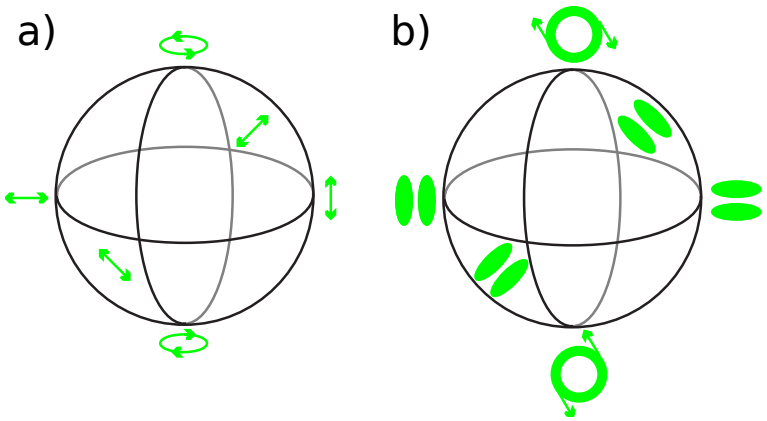

Fig. 1. The superposition of polar states giving equatorial states with an orientation dependent on the relative phase between the polar states for (a) a Poincaré sphere for SAM and (b) a Bloch sphere for OAM.

In addition to SAM, light carries another form of angular momentum, which is known as

#206677 - $15.00 USD Received 18 Feb 2014; revised 30 Mar 2014; accepted 23 Apr 2014; published 7 May 2014

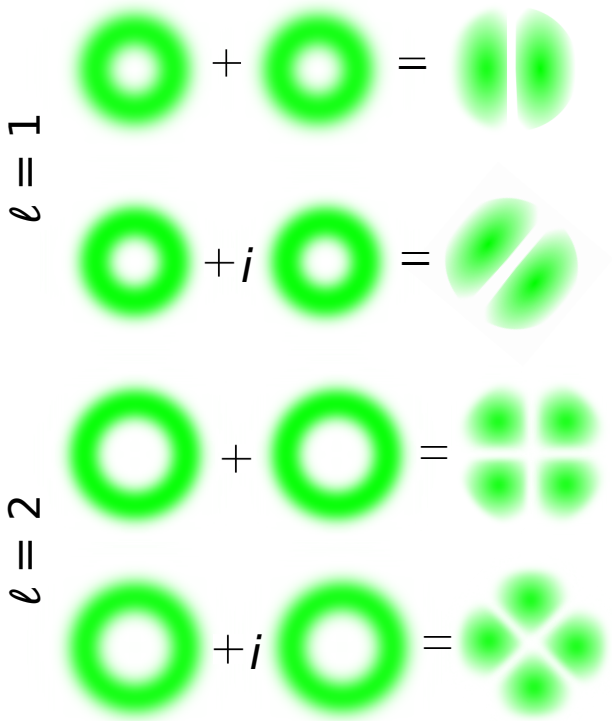

Fig. 2. Petal patterns created by a superposition of $\pm\ell$ beams. The second and fourth lines have a phase shift, i, between the $+\ell$ and $-\ell$ beams, causing a 45 degree rotation of the petal pattern.

orbital angular momentum (OAM) and has been studied in detail for the last 20 years [8, 9]. Beams carrying OAM, such as Laguerre-Guassian (LG) beams, have a Poynting vector with an azimuthal component that corresponds to phase fronts with a helical structure [8], rather than plane waves. Helical phase fronts are described by $\exp(i\ell\phi)$ and carry OAM of $\pm\ell\hbar$ per photon, where ℓ is an integer and ϕ is the angular coordinate. Just as the superposition of right- and left-handed circularly polarised light creates linearly polarised light, a superposition of two LG beams with $\pm\ell$ gives rise to a petal pattern with 2ℓ petals. Interfering positive ℓ and negative $(\ell+1)$ LG beams results in $2\ell+1$ petals, allowing us to examine odd petal patterns as well as even ones. A change in the relative phase between the LG beams causes a rotation of the petal pattern. Analogous to the Poincaré sphere for polarisation is a Bloch sphere, which can be constructed for OAM using LG beams with $\pm\ell$ as the polar states [10]. The Bloch sphere for LG beams with $\ell = \pm 1$ is shown in Fig. 1(b), where the states lying along the equator are Hermite-Gaussian (HG) states with orientations dependent on the relative phase of the $\pm\ell$ polar states. Figure 2 shows the superposition of $\ell = \pm 1$ and $\ell = \pm 2$ resulting in two and four petals respectively, with phase shifts being introduced to show the rotation of the petal pattern in the second and fourth cases. The mechanical Faraday effect, which is related to SAM and rotates the polarisation state of the light, also rotates the image and is related to OAM.

As discussed and demonstrated by Jones [7, 11] and then expanded by many others [5, 6, 12, 13], when light enters a translating medium, it is dragged by that medium. By applying well-

#206677 - $15.00 USD Received 18 Feb 2014; revised 30 Mar 2014; accepted 23 Apr 2014; published 7 May 2014

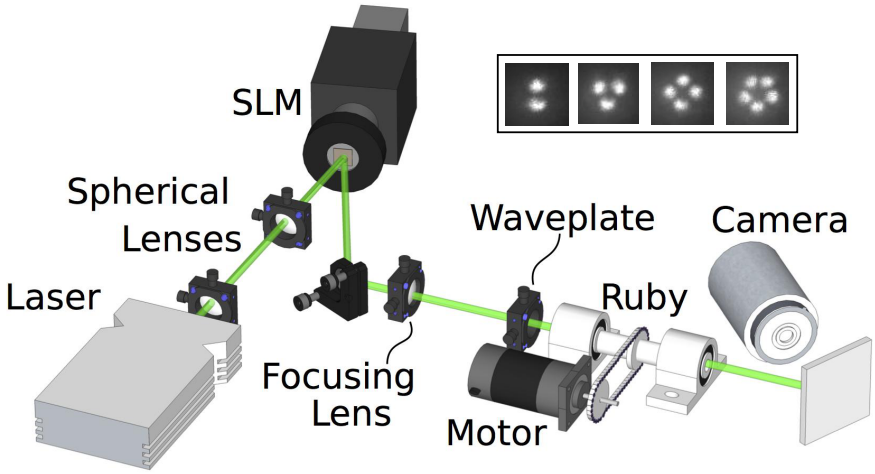

Fig. 3. 532 nm light passes through two spherical lenses to be expanded before arriving at the spatial light modulator (SLM). The beam is then focused onto the front face of a ruby window, which is spun about its axis by a motor. The light is imaged from the back of the ruby onto a screen and then captured by a camera. Petal patterns are made from superpositions of LG beams with different l values while the ruby window spins at ± 19 Hz. Patterns shown in the inset are (from left to right) 2 petals from $l = \pm 1$; 3 petals from $l = (+1, -2)$; 4 petals from $l = \pm 2$; and 5 petals from $l = (+2, -3)$.

known formulas for transverse drag in a rotating medium, Padgett et al. [4] predicted the angle through which an image should be rotated and found that the polarisation state and the image are dragged through the same angle, which implies some equivalence between SAM and OAM.

Making this reasonable but unproven assumption that SAM and OAM are subject to the same phase change, we see that the image is dragged by the moving medium through an angle

$$\Delta\theta = \left(n_g - \frac{1}{n_\phi}\right)\frac{\Omega L}{c}, \tag{1}$$

where n_g and n_ϕ are the group and phase indices of the medium, Ω and L are the rotational speed and the length of the medium, and c is the speed of light in a vacuum [4, 12]. In most media, the speed of light is much larger than $\Omega L n_g$. The transit time of light through the medium is then very short, which leads to a small angle of dragging. To increase the angle of rotation, we increase the transit time of the light through the medium. As there is a physical limit to the experimentally realistic length of the medium, the practical method for increasing transit time is to use a slow-light medium. When the light passes through a slow-light medium, the transit time increases such that there is a large angle of dragging [14, 15]. The rotation of polarisation was measured in 1976 by Jones [7]. However image rotation proved much harder to detect, with the first observation of image rotation occurring 35 years later by using the enhancing effect of a rotating slow-light medium [16]. Slow light is a complicated phenomenon whose mechanism has been the subject of much debate (see [17] for a review of slow-light research). Whereas previous research has investigated more broad questions about general rotational drag [18–20], this research investigates the rotation of specific superpositions of LG beams by a rotating medium.

In order to examine the effect of a rotating medium on an OAM-carrying beam, an 18 W single-mode Verdi laser creates a beam of intense 532 nm laser light. The beam is expanded by

#206677 - $15.00 USD Received 18 Feb 2014; revised 30 Mar 2014; accepted 23 Apr 2014; published 7 May 2014

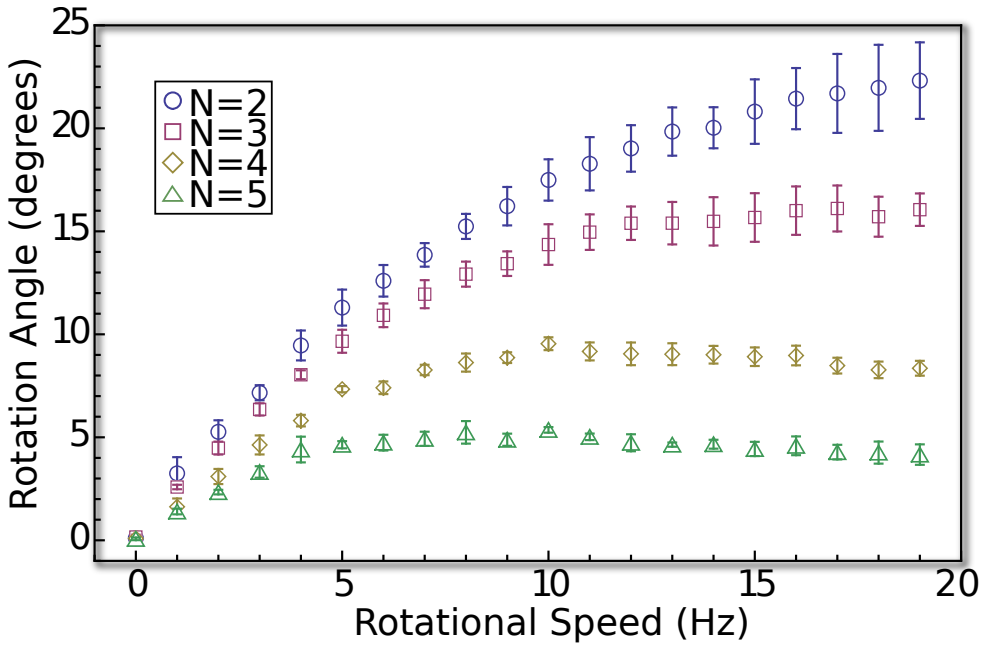

Fig. 4. Rotation angle of petal patterns with $N = 2$ through 5 petals as a function of rotational speed while held at constant peak intensity. Patterns with different N saturate at different rotational speeds. Error bars represent the standard deviations of independent data runs.

two spherical lenses with focal lengths of 20 mm and 80 mm, and the expanded beam is incident upon a Hamamatsu spatial light modulator (SLM). The SLM creates the desired pattern with careful control of both the phase and intensity of the light. In our experiment, the SLM creates petal patterns from the superposition of two opposite handed LG modes, as shown in Fig. 2 for 2 and 4 petals, where the number of petals (N) is given by the difference in the azimuthal mode index of the two beams. In order to interact evenly with the birefringent ruby crystal as it spins, the beam passes through a $\lambda/4$ waveplate to create circularly polarised light. The beam is focused down onto the front face of a standard laser ruby crystal (diameter = 10 mm, length = 90 mm) by a 300 mm focal length spherical lens, as shown in Fig. 3.

A stepper motor couples to the ruby mount, and the motor spins the ruby window about its axis up to $\approx \pm 20$ rotations per second. We use a standard desktop computer to control both the direction and rate of rotation of the ruby. The light is imaged from the back face of the ruby onto a screen, and a camera collects the image to display on a monitor. We use standard National Instruments IMAQ pattern matching software to compare the image under clockwise rotation to that obtained from anticlockwise.

All our reported results relate to intensity patterns formed from the superposition of two beams with OAM indices ℓ_1 and ℓ_2, resulting in rotationally symmetric patterns with $N = |\ell_1| + |\ell_2|$ petals, i.e. with N-fold symmetry. In all cases, we report the rotation angle, which is measured by the difference in orientation obtained between clockwise and anticlockwise rotation of the ruby through which the pattern is transmitted.

Figure 4 shows the rotation angle of the petal patterns as a function of rotation speed for various numbers of petals. Because the petal patterns are slightly different sizes, the peak intensity in each pattern varies for constant input laser power. To overcome this problem, the laser power

#206677 - $15.00 USD Received 18 Feb 2014; revised 30 Mar 2014; accepted 23 Apr 2014; published 7 May 2014

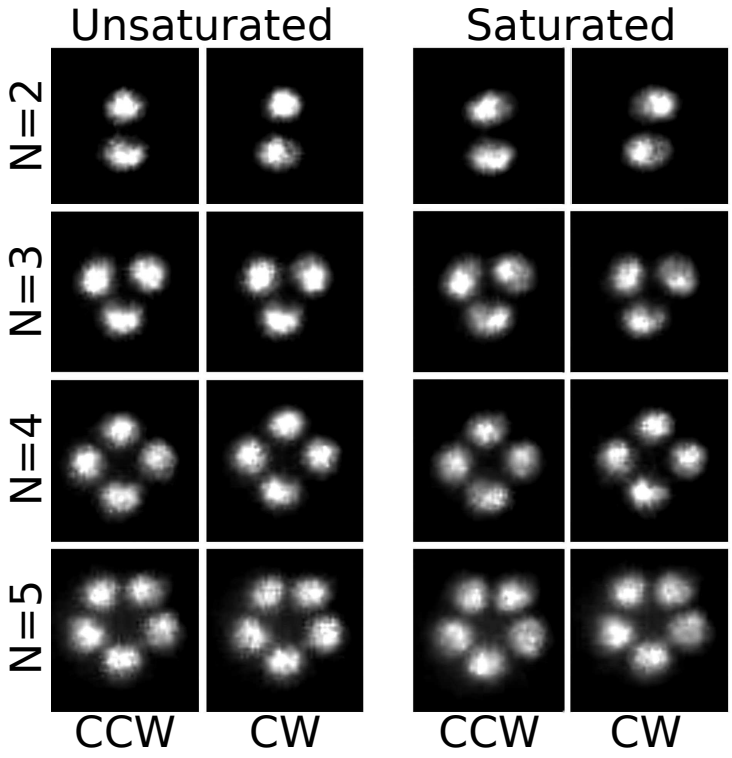

[h!]

Fig. 5. Images of N =2-5 for unsaturated (low rotational frequency, first column) and saturated (high rotational frequency, second column) modulation frequencies with the ruby spinning counterclockwise (CCW) and clockwise (CW).

was adjusted between patterns such that the peak intensity was held constant. The laser power was set to 3.90 W, 4.30 W, 4.68 W, and 5.16 W, for N =2, 3, 4, and 5, respectively, to result in constant peak intensities in all four patterns. The experiment was conducted multiple times, resulting in independent measurements that were averaged to achieve the most accurate rotation angles. Errors were calculated by measuring the standard deviation between independent data collections at each point and are shown in Figs. 4 and 6. Errors are not constant, due to the minor image distortion upon rotation that affected some points more than others.

Firstly, we note that in all cases an increase in N reduces the rotation angle of the pattern. Secondly, we note that the linear increase in the rotation angle with speed holds only up to a certain point, after which the angle tends to saturate, and that this saturation occurs at lower speeds for higher N. Neither of these trends is in simple agreement with the Jones expression that, by contrast, predicts that the rotation angle increases linearly with rotational speed and should be unchanged by the symmetry of the pattern. For any given setup, Jones assumes a constant n_g, but in our slow-light system, n_g is a complicated function of the experimental parameters, as described below.

These two deviations from the behaviour described by the Jones's equation (Eq. (1)) can be understood in terms of the nature of the slow-light effect. In the original slow-light experiments

#206677 - $15.00 USD Received 18 Feb 2014; revised 30 Mar 2014; accepted 23 Apr 2014; published 7 May 2014

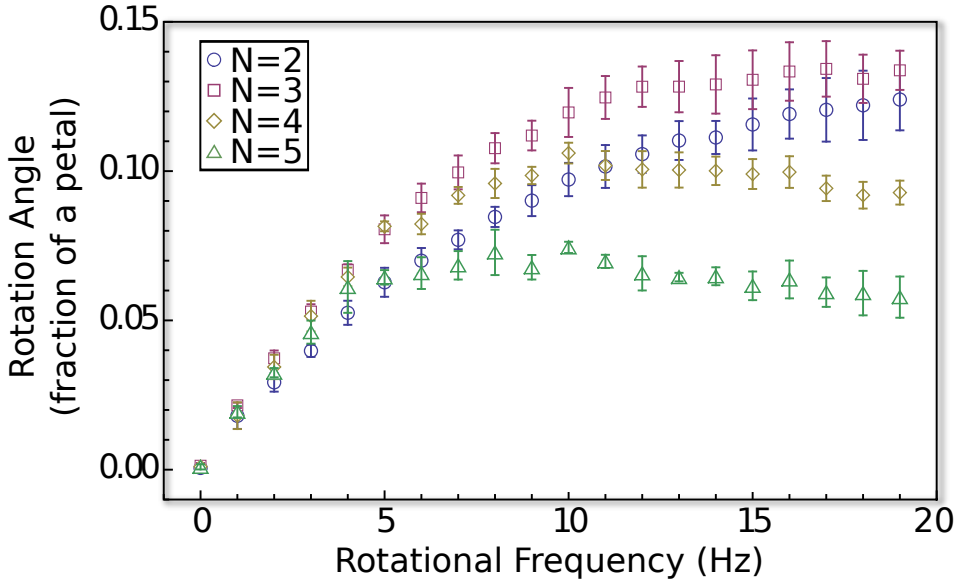

Fig. 6. Fraction of a petal rotated by $N = 2$ through 5 petals as a function of rotational speed while held at constant peak intensity. Error bars represent the standard deviations of independent data runs.

in ruby, the slowing of the light was manifest by the time delay in the sinusoidally modulated intensity of a beam of light [14]. The slowing was largest when the modulation frequency was small compared to the ≈ 4 millisecond upper-state lifetime of the ruby (corresponding to the metastable $2\overline{A}$ and $\overline{E}$ levels). We note that, in our rotational case, the ruby is also subject to a modulated intensity at a frequency equal to the rotation rate of the medium multiplied by the number of petals in the beam. That is to say, each time a given part of the ruby crystal rotates into the position of a bright petal, it will be subject to a high optical intensity, which results in an intensity modulation that depends upon both the rotational frequency of the ruby and N, the petal number. For example, when the ruby is rotating at 10 Hz and is illuminated by a $N = 2$ pattern, each atom in the ruby will experience a fluctuation in the optical intensity at 20 Hz. We note that the change in the rotation speed at which the saturation occurs is consistent with this N-dependent modulation frequency, namely that the saturation frequency scales with the reciprocal of the number of petals. Whereas $N = 2$ saturates at ≈ 20 Hz, $N = 3$ saturates at ≈ 13 Hz, $N = 4$ at ≈ 10 Hz, and $N = 5$ at ≈ 8 Hz, resulting in a modulation frequency of approximately 40 Hz for all four cases. Representative images are shown in Fig. 5 for N =2 through 5 in both the unsaturated (low frequency) and saturated (high frequency) while the ruby is rotating counterclockwise and clockwise.

As seen in Fig. 4, at a given rotational speed, patterns with more petals rotate through a smaller angle than patterns with fewer petals. Instead of plotting the angle through which the pattern is rotated, we instead plot the fraction of a petal rotated as a function of speed. Figure 6 shows that all of the patterns rotate less than 0.15 petals, where 1.0 petal would rotate the pattern by 360deg./N, resulting in an identical pattern. It appears that increasing the number of petals will not result in a pattern that will completely rotate a petal into an area of darkness, which would correspond to a rotation of 0.5 petals. Irrespective of the number of petals or rotation speed and due to the complicated nature of the slow-light effect, the maximum rotation in this

#206677 - $15.00 USD Received 18 Feb 2014; revised 30 Mar 2014; accepted 23 Apr 2014; published 7 May 2014

experimental configuration is restricted to be less than the distance characterised by the spatial structure of the beam.

Theories on slow light in ruby are highly contentious [21, 22], falling primarily into two models. The first model describes the phenomenon entirely through simple pulse reshaping and states that slow light is not required to explain the observed effects [23]. The second model describes slow light as the process of coherent population oscillations, where the degree of slowing is a complicated function of the functional form of the light field [17]. Our results may be used to inform the debate on slow light in ruby. Any successful model would need to account for the results of this experiment. The key features of this experiment are that the effect saturates with the modulation frequency, which is a product of the spatial feature of the beam profile and the rotation frequency, and that no petal pattern can rotate through a full spatial feature of the beam profile. Our results also show some evidence that all petal patterns rotate through the same angle at low frequencies (see the low frequency region of Fig. 6).

We have shown the rotation of OAM-carrying beams that is analogous to the polarisation rotation related to SAM. The rotation of OAM-carrying beams appears to be limited to a fraction of a petal, implying an inability to rotate a petal pattern by the angular extent of a petal, regardless of the number of petals in the beam. These results highlight the complex nature of slow light in the mechanical Faraday effect for OAM-carrying beams and provide experimental evidence against which theories of slow light in ruby can be measured.

Acknowledgments

This work was supported by the Engineering and Physical Sciences Research Council [grant number EP/I012451/1]. E.L.W.-B. is supported by the Scottish Universities Physics Alliance, and M.J.P. is supported by the Royal Society. R.W.B. gratefully acknowledges support by the US Defense Threat Reduction Agency and the Canadian Excellence Research Chairs programme.

#206677 - $15.00 USD Received 18 Feb 2014; revised 30 Mar 2014; accepted 23 Apr 2014; published 7 May 2014